# Crystallisation Kinetics of Metal Organic Frameworks

# From *in situ* Time-Resolved X-ray Diffraction

Racha El Osta[1], Mark Feyand,[2] Norbert Stock,[2] Franck Millange[1*] and Richard I. Walton[3*]

*author for correspondence, email: r.i.walton@warwick.ac.uk or franck.millange@uvsq.fr

1. Institut Lavoisier Versailles, Université de Versailles, UMR 8180, 78035 Versailles, France

2. Institut für Anorganische Chemie, Christian-Albrechts-Universität, Max-Eyth-Straße 2, D-24118 Kiel, Germany.

3. Department of Chemistry, University of Warwick, Coventry, CV4 7AL, UK

A time-resolved powder diffraction study of the crystallisation of porous metal organic framework materials with the CPO-27 structure ($[M_2(dhtp)(H_2O)_2]\cdot 8H_2O$ where, dhtp = 2,5-dioxoterephthalate) using the energy dispersive X-ray diffraction method is described. Crystallisation under solvothermal conditions is performed between 70 - 110 °C from clear solutions of metal salts (M = $Co^{2+}$ or $Ni^{2+}$) and 2,5-dihydroxyterephthalic acid in a mixture of THF-water in sealed reaction vessels, using both conventional and microwave heating. Integration of Bragg peak areas with time provides accurate crystallisation curves, which are modelled using the method of Gualtieri to determine rate constants for nucleation and for growth and then, by Arrhenius analysis, activation energies. Crystallisation is determined to be one-dimensional, consistent with the elongated morphology of the crystals produced in these reactions. With conventional heating the Co-containing CPO-27 crystallises more rapidly than the isostructural Ni-containing analogue and analysis of the kinetic parameters would suggest a complex multi-step crystallisation process. The effect of microwave heating is upon activation energies: the values for both nucleation and for crystal growth are lowered compared to reactions using conventional heating.

Key words: Metal Organic Frameworks, Energy Dispersive, Time Resolved, X-ray Diffraction



https://doi.org/10.1017/S0885715613000997 Published online by Cambridge University Press

## I. INTRODUCTION

Metal-organic framework (MOF) materials are a large, and growing, family of hybrid organic-inorganic solids that are the focus of intense investigation at present (Long and Yaghi, 2009; Kepert, 2010; MacGillivray, 2010; Farrusseng, 2011). The concept behind MOF structural chemistry is simple: the combination of metal ions, or clusters of metal ions, with polydentate ligands to yield extended structures whose topology is defined by the coordination preference of the metal and the connectivity, size and shape of the organic 'linkers' (Yaghi *et al.*, 2003). In many cases this approach yields open-framework, three-dimensional structures that may possess considerable porosity, once any trapped solvent or unreacted ligand is removed. MOFs represent a new generation of porous solids that have the potential to extend the well-known applications of materials such as zeolites and mesoporous silicas (in separation, catalysis and sensing) into new directions (Czaja *et al.*, 2009). Despite their lower thermal stability compared to solely inorganic framework solids, of particular, fundamental interest is the use of MOFs for gas adsorption, making use of their exceptional porosity and the potential for strong interactions with coordinatively unsaturated framework metals or ligands of suitable design, in important applications such as hydrogen storage (Murray *et al.*, 2009) or $CO_2$ capture (Sumida *et al.*, 2012). MOFs are also attracting interest for a variety of other reasons, including for the storage and release of biologically active molecules (Horcajada *et al.*, 2012), for the realisation of chiral, porous hosts (Yoon *et al.*, 2012) and for the large structural flexibility that some exhibit (Férey and Serre, 2009).

In order to realise the potential of MOFs it is desirable to have some degree of predictability in their synthesis, and this requires the need for a detailed understanding of their crystallisation kinetics and mechanisms: i.e., the fundamental steps in the assembly of complex extended structures from dissolved precursors or reorganisation of gel phases mediated by solvent, and the relative rates of reaction of each step involved. This is a challenging problem, well-known from zeolite chemistry (Barrer, 1982; Cundy and Cox, 2003), where the observation of crystallisation in a sealed solvothermal reaction vessel requires the careful design of experiments that probe some change of physical property as reaction proceeds (Francis and O'Hare, 1998; Walton *et al.*, 1999a). Study of material quenched from reaction at various times may give rudimentary information about the course of crystallisation, but makes the significant



https://doi.org/10.1017/S0885715613000997 Published online by Cambridge University Press

assumption that no irreversible change has occurred on removing the material; hence *in situ* studies are needed to follow properly the formation of product. There is probably no single experiment that allows chemical order over all lengths scales to be monitored simultaneously, and indeed both spectroscopic and diffraction methods have been applied to obtain the information required (Cheetham and Mellot, 1997; Walton and O'Hare, 2000; Pienack and Bensch, 2011).

In the case of MOFs only in the past few years have results from the *in situ* study of their crystallisation been reported; this includes *in situ* diffraction studies that have revealed the first quantitative information concerning the kinetics of crystallisation of some prototypical MOFs and the observation of metastable phases that have short lifetimes under solvothermal conditions (Millange *et al.*, 2010; Stavitski *et al.*, 2011). Other techniques that have been used to monitor MOF crystallisation include light scattering, which reveals information concerning the growth and decay of precrystallisation agglomerates in reaction solution (Zacher *et al.*, 2009), and atomic force microscopy that provides information about layer by layer surface growth of crystallites (Shoaee *et al.*, 2008).

Herein we describe some new results obtained from an *in situ* powder X-ray diffraction study of the crystallisation of large-pore MOF materials with the CPO-27 structure. CPO-27, $[M_2(dhtp)(H_2O)_2]\cdot 8H_2O$, is constructed from $M^{2+}$ centres connected by the multidentate linker 2,5-dioxoterephthalate (dhtp) to yield a three-dimensional structure with one-dimensional channels that have approximately circular openings of diameter ~ 11 Å (Dietzel *et al.*, 2010), Figure 1. The metals are found in octahedral coordination, in edge-shared dimers further linked by shared corners, in which one of the vertices is terminally attached solvent (water or alcohol) that may be removed by thermal or vacuum treatment to yield coordinatively unsaturated metal sites. Isostructural frameworks are known for a variety of $M^{2+}$ ions, including Ni, Fe, Mg, Co, Mn and Zn (in the latter case the framework is also known as MOF-74 (Rosi *et al.*, 2005), and the materials have been studied for their useful properties in gas adsorption, for example, for dihydrogen (Dietzel *et al.*, 2010), $H_2S$ (Allan *et al.*, 2012), selective binding of oxygen over nitrogen (Bloch *et al.*, 2011), and various toxic gases (Glover *et al.*, 2011). In this paper we describe an analysis of the kinetics of crystallisation of two of these materials, CPO-27(Ni) and CPO-27(Co), and we compare the results with the so-far described kinetic studies of MOF



https://doi.org/10.1017/S0885715613000997 Published online by Cambridge University Press

crystallisation available in the literature. We have used the method of energy dispersive X-ray diffraction (EDXRD), which offers a convenient method of measuring powder diffraction patterns from within a sealed reaction vessel, due to the high intensity white X-ray beam, with fast data collection (of around 1 minute per diffraction pattern) because of the fixed-angle solid-state detector (Walton and O'Hare, 2000). EDXRD is a proven method for probing the crystallisation kinetics of a variety of materials under solvothermal conditions, from microporous zeotype materials (Munn *et al.*, 1992; Sankar *et al.*, 2007; Walton *et al.*, 1999b; Walton *et al.*, 2001) and open-framework phosphonates (Feyand *et al.*, 2010; Schmidt and Stock, 2012; Schmidt *et al.*, 2012; Feyand *et al.*, 2012 ), to metal oxides (Croker *et al.*, 2009; Kiebach *et al.*, 2008; Modeshia *et al.*, 2009) and metal sulfides (Francis *et al.*, 1996; Kiebach *et al.*, 2006), and also has been used to follow the intercalation of guest molecules into layered hosts (O'Hare *et al.*, 2000).

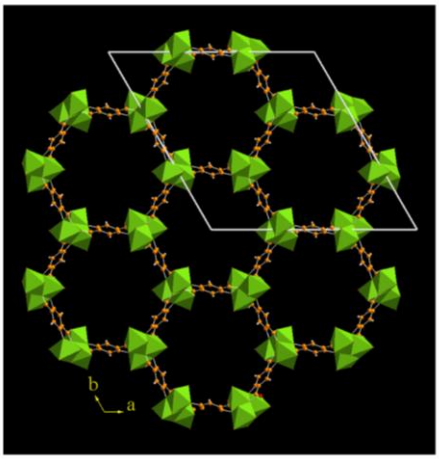



Figure 1: View of the structure of desolvated CPO-27 structure parallel to the 1D channels.

## II. EXPERIMENTAL

*In situ* EDXRD data were recorded during the crystallisation of CPO-27 materials using Beamline F3 of the HASYLAB facility, Germany. This beamline received white-beam radiation with energy 13.5 – 65 keV and the incident X-ray beam on the sample was collimated to 20 × 20 $\mu m^2$. EDXRD patterns were accumulated using a fixed-angle solid-state germanium detector. Reactions were performed with 12 mm diameter DURAN® tubes fitted with PBT screw caps and PTFE-coated gaskets. 2 mL of the clear solution of reagents were placed into the reaction tube which was immediately transferred into a circulating oil heater equipped with a magnetic



https://doi.org/10.1017/S0885715613000997 Published online by Cambridge University Press

stirring device. Microwave assisted EDXRD studies were carried out in a Biotage Initiator microwave reactor system with custom modification to allow the beam to pass the microwave chamber and irradiate the glass vessel directly. The temperature within the microwave vial was measured by a IR sensor and the reactions were stirred continually through the study at a similar speed to the conventional heating experiments. The power of the microwave was controlled remotely to hold the desired temperature.

For the synthesis of CPO-27 materials, 0.937 g Ni acetate (or 0.938 g Co acetate) was dissolved in 25 ml of deionised water and separately 0.372 g 2,5-dihydroxyterephthalic acid was dissolved in 25 ml of tetrahydrofuran. In the reaction tube 1 ml of each solution was mixed to give a clear solution, which was immediately sealed and transferred to the heating device. EDXRD patterns were recorded in 120 s intervals using the Ge detector whose angle (2θ) was calibrated using the characteristic Bragg peaks of a pre-made solid sample of CPO-27(Ni). In the EDXRD experiment, each Bragg peak is characterised by an energy, *E*/keV, related to its *d*-spacing, *d*/Å, according to Eq. 1.

$$E = \frac{6.1992}{d\sin\theta} \tag{1}$$

The raw EDXRD data were normalised to the incident beam intensity by using the logged synchrotron beam current, and Bragg peak integration was performed using the software f3tool (Rothkirch, 2009). The identification of the final solid product was also confirmed using *ex situ* high-resolution powder XRD. Each crystallisation run was repeated at least on three occasions during several visits to Beamline F3 to check for consistency in the data.

Kinetic analysis was performed using least-squares refinement to the equations derived by Gualtieri for the crystallisation of aluminosilicate zeolites under hydrothermal conditions (see below), within the software (OriginLabCorp 1991-2010). The products from the reactions studied *in situ* were recovered by suction filtration, dried and retained for later analysis using scanning electron microscopy. This was performed using a JEOL JSM-7001F FEG scanning electron microscope.

## III. RESULTS AND DISCUSSION



https://doi.org/10.1017/S0885715613000997 Published online by Cambridge University Press

Figure 2 shows a 3D contour plot of a typical CPO-27 crystallisation. In the energy window studied, two characteristic Bragg peaks are observed to form soon after starting the measurement, following only a short induction time, which is only apparent at the lowest temperatures used. Figure 3 shows crystallisation curves as a function of temperature for Ni(II) and Co(II) containing CPO-27 determined by integration of the most intense (-120) Bragg peak of each phase. It is immediately apparent that the crystallisation of the Ni form of CPO-27 is retarded compared to the Co analogue, with, for example, the time for crystallisation to reach completion for CPO-27(Ni) at 110 $^{o}$C being approximately the same for CPO-27(Co) at 90 $^{o}$C. The induction times for crystallisation are very similar in each case, and crystallisation begins within a few minutes of heating. This is consistent with the previous observations of Haque and Jhung who studied the crystallisation of the same materials from DMF-water mixtures and, by quenching and powder diffraction analysis of the products, derived approximate crystallisation curves (Haque and Jhung, 2011). They proposed that the higher lability of $[Co(H_2O)_6]^{2+}$ was responsible for its enhanced rate of reaction with the carboxylate ligand via increased solvent-ligand exchange kinetics.

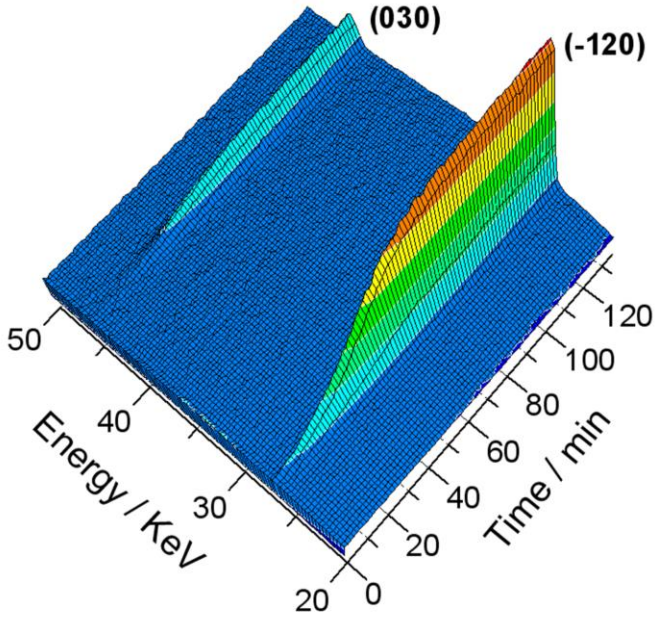



Figure 2: A 3D contour plot of the EDXRD data recorded during the crystallisation of CPO-27(Ni) at 90 °C.



https://doi.org/10.1017/S0885715613000997 Published online by Cambridge University Press

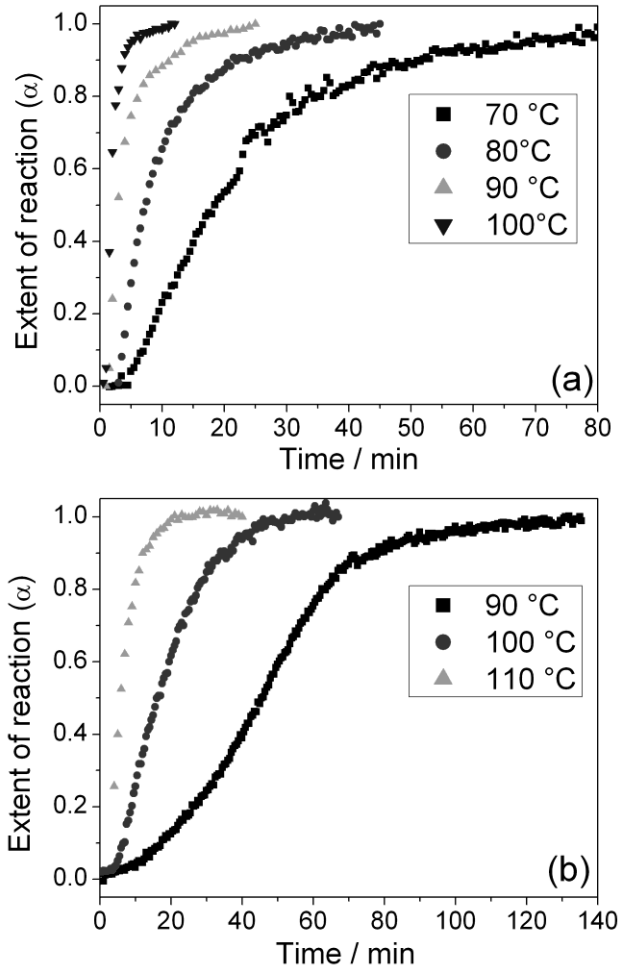



Figure 3: Crystallisation curves as a function of temperature for (a) CPO-27(Co) and (b) CPO-27(Ni) determined by integration of the (-120) Bragg peak of each phase.

For analysis of our new crystallisation curves, in order to obtain quantitative kinetic information concerning crystallisation, we have used the method of Gualtieri, who studied the crystallisation of aluminosilicate zeolites and derived an expression for the crystallisation kinetics (Gualtieri, 2001). This model provides a mathematical description based on nucleation-growth crystallisation and the advantage of using this model for simulating crystallisation is that it separates nucleation and growth into two processes, each with separate rate constants. We and others have recently applied the Gualtieri model to crystallisation data from a number of metal-organic frameworks (Cravillon *et al.*, 2012; El Osta *et al.*, 2012; Millange *et al.*, 2011; Reinsch and Stock, 2012), and this current study provides the opportunity to compare the calculated kinetic parameters between different MOF crystallisations to gain some greater physical insight into crystallisation.



https://doi.org/10.1017/S0885715613000997 Published online by Cambridge University Press

The Gualtieri model describes crystallisation according to Eq. 2.

$$\alpha = \frac{1}{1 + \exp\left\{-\left(\frac{t-a}{b}\right)\right\}}\left\{1 - \exp\left[-\left(k_g\right)^n\right]\right\} \tag{2}$$

This expression shows how the extent of crystallisation (normalised from zero to one), α, is related to *t*, the time coordinate of the crystallisation, to the parameters $k_g$, the rate of crystal growth, *a* and *b*, constants that parameterise nucleation, and *n* the dimensionality of crystal growth (which may be determined by independent observations, such as crystal morphology from electron microscopy and by consideration of the crystal symmetry of the material being studied). By fitting this expression against the experimentally determined extent of crystallisation, the probability of nucleation, $P_N$, can then be calculated using Eq. 3.

$$P_N = exp\left\{-\frac{(t-a)^2}{2b^2}\right\} \tag{3}$$

The rate of nucleation, $k_n$, is then defined as $1/a$. The parameter *b* is believed to contain information about the crystal growth mechanism (see below).

Figures 4 and 5 show fits obtained by fitting of the Gualtieri model to the crystallisation data of CPO-27(Co) and CPO-27(Ni), respectively, using a least squares fitting procedure. It is important to note that in order to obtain a physically meaningful set of rate constants (increasing with reaction temperature) the value of *n* was required to be equal to 1 and hence was fixed to determine final refined values of the other parameters. This implies a one-dimensional crystal growth, which is entirely consistent with the needle-like crystals previously reported for CPO-27 materials (Haque and Jhung, 2011), and the SEM images recorded from our samples, Figure 6, that show a distinctive elongated morphology. Note that we have studied crystallisation curves derived from integration of the most intense (-120) Bragg peaks so this analysis may suggest that the long axis of the crystals lies in this direction.



https://doi.org/10.1017/S0885715613000997 Published online by Cambridge University Press

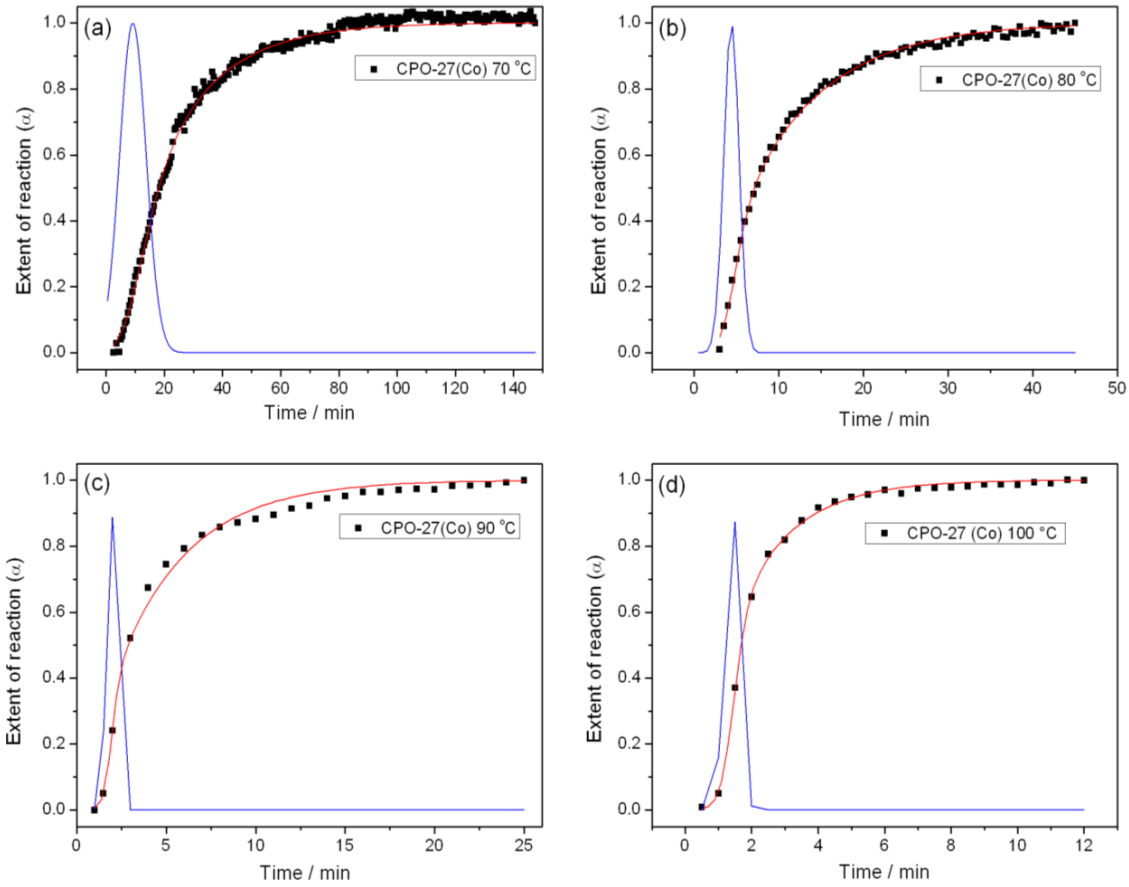



Figure 4: Fits obtained by fitting to the Gualtieri model to CPO-27 crystallisations for CPO-27(Co) at (a) 70 °C (b) 80 °C (c) 90 °C and (d) 100 °C.



https://doi.org/10.1017/S0885715613000997 Published online by Cambridge University Press

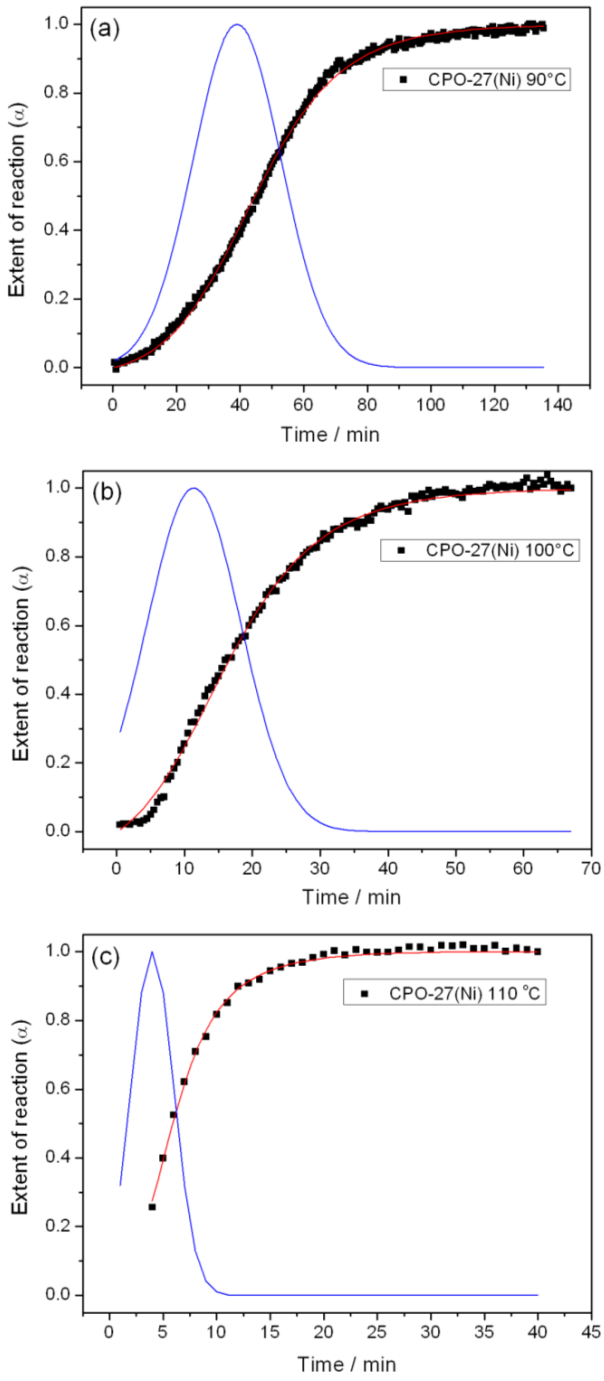



Figure 5: Fits obtained for fitting to the Gualtieri model to CPO-27 crystallisations for CPO-27(Ni) at (a)90 °C, (b) 100 °C and (c) 110 °C.



https://doi.org/10.1017/S0885715613000997 Published online by Cambridge University Press

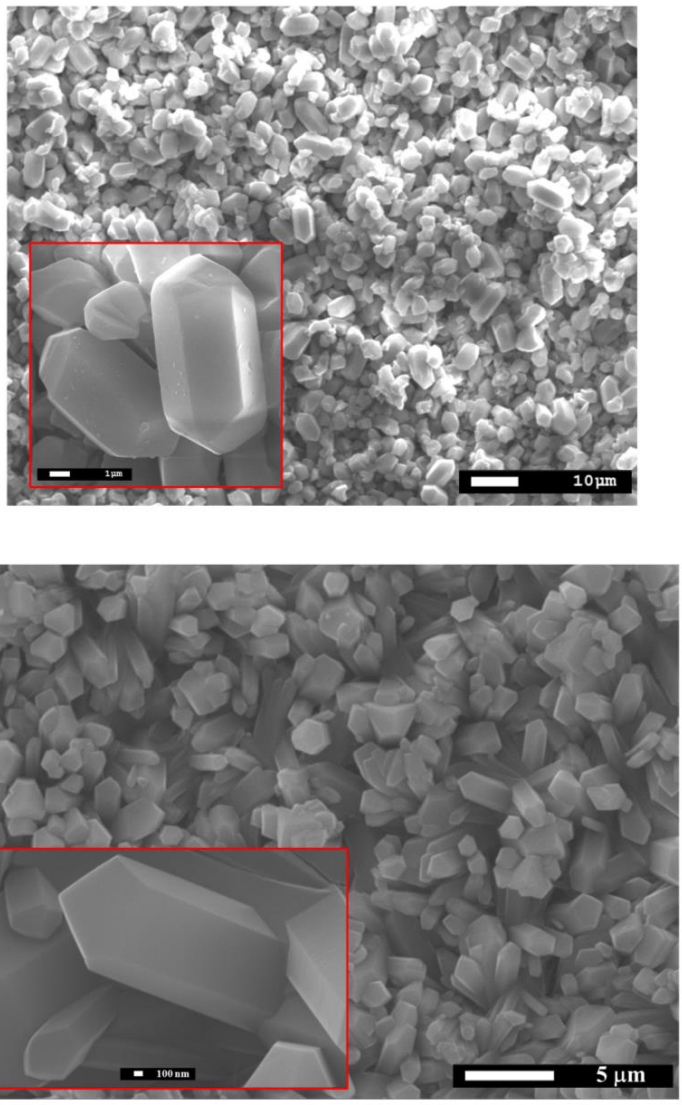



Figure 6: SEM images of typical samples of (a) CPO-27(Co) and, (b) CPO-27(Ni) prepared using conventional heating.

Table I contains the fitted kinetic parameters. According to the Gualtieri model the parameter *b* contains information relating to the mechanism of crystal growth; in the original work the *b* value was compared to other kinetic models for crystallisation to distinguish between three types of crystallisation: homogeneous, heterogeneous and autocatalytic (Gualtieri, 2001). For values of *b* less than 15, it is suggested that crystallisation occurs via a heterogeneous pathway, meaning, for example, crystallisation takes place at preformed aggregates in the reaction mixture. It is interesting to note that the *b* values, Table I, show a distinctive positive temperature dependence for both CPO-27(Ni) and CPO-27(Co). This would suggest that the crystallisation actually proceeds via at least two distinct steps and the



https://doi.org/10.1017/S0885715613000997 Published online by Cambridge University Press

effect of temperature changes the limiting step, switching the dominant (i.e., rate determining) step.

Table 1: Fitted kinetic parameters for crystallisation of CPO-27(Ni) and CPO-27(Co) from Gualtieri analysis of crystallisation curves. See Equations 2 and 3 in the text for definitions of the parameters.

| **Material** | **Temperature / $^{o}$C** | ***a* / min** | ***b* / min** | ***kg/min-1*** | ***kn/min-1*** |
|---|---|---|---|---|---|
| CPO-27(Ni) | 90 | 30.04(34) | 13.86(16) | 0.041(1) | 0.0333(4) |
| | 100 | 11.38(34) | 6.92(25) | 0.080(3) | 0.0879(26) |
| | 110 | 4.00(13) | 1.98(15) | 0.199(7) | 0.2500(81) |
| CPO-27(Co) | 70 | 9.17(25) | 4.52(23) | 0.04673(4) | 0.1091(30) |
| | 80 | 4.37(6) | 0.90(5) | 0.1049(7) | 0.2288(31) |
| | 90 | 1.88(5) | 0.23(6) | 0.247(6) | 0.532(14) |
| | 100 | 1.394(15) | 0.205(14) | 0.586(8) | 0.7174(77) |

In Table II we compare the activation energies for both crystal growth and nucleation, determined from Arrhenius plots, as shown in Figure 7, with values reported in the literature for other metal-organic framework materials whose solvothermal crystallisation has also been analysed using the Gualtieri model. It is interesting to observe that, while the activation energies of crystal growth for both CPO-27(Co) and CPO-27(Ni) are virtually the same (~ 90 kJ mol$^{-1}$), the activation energy for nucleation for the Ni material is approximately double that of the Co material. The CPO-27(Co) also shows a smaller activation energy for nucleation than for crystal growth. Both observations may reflect the greater lability of hydrated $Co^{2+}$ over hydrated $Ni^{2+}$, such that the initial replacement of bound water by the ligand occurs rapidly to initiate the formation of nucleation sites for subsequent crystal growth. This would be consistent with the conclusions of the quenching studies of Haque and Jhung (Haque and Jhung, 2011). Our kinetic analysis also shows that the simulated nucleation curves do not extend far into the crystallisation period, suggesting that early formation of nucleation sites is followed by a longer period of crystallisation (note that the structure of CPO-27 contains edge- and corner-shared metal-centred octahedra so the assembly of the structure is more complex than simply replacing the bound water by bridging



https://doi.org/10.1017/S0885715613000997 Published online by Cambridge University Press

ligands). The larger size of the CPO-27(Co) crystals that are formed confirms independently the observations from fitting the kinetic data; *i.e.*, since nucleation is more rapid than for the Ni analogue, a more extended period of crystal growth at the nucleation sites can take place.

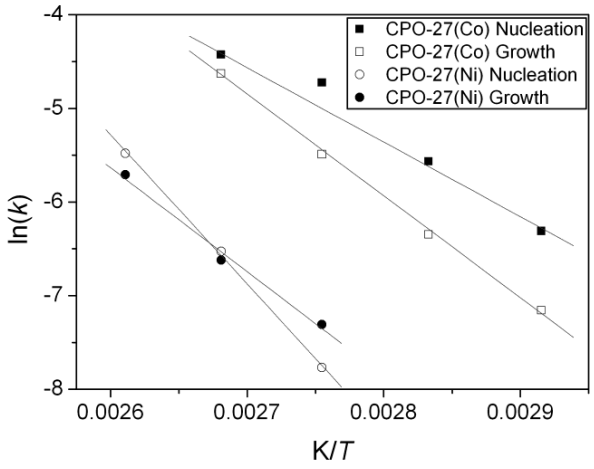



Figure 7: Arrhenius plots for nucleation and for growth obtained for the crystallisation of CPO-27(Co) and CPO-27(Ni). The lines are fits obtained by linear regression.

Table II contains data from materials that show both one- and three-dimensional crystal growth and correspondingly yield crystals of elongated or isotropic form, respectively. The activation energies both for nucleation and for crystal growth all fall between 60 and 140 kJ $mol^{-1}$ but the relative size within each pair of values for a given crystallisation varies quite noticeably. For the cases of three-dimensional crystal growth, leading to crystals with isotropic morphology, the two copper-containing MOFs MOF-14 and HKUST-1 show instantaneous nucleation (crystallisation commences as soon as the reagents are mixed), but nucleation controlled reactions (the activation energy for nucleation is larger than for crystal growth and nucleation extends well into the crystallisation period) (Millange *et al.*, 2011). In the study of ZIF-8 crystallisation by Cravillon *et al.*(2012) where a short induction time for crystallisation was observed, the activation energies for nucleation and crystal growth are almost equal. It should be noted in that work that the addition of formate to the reagent mixture was used to accelerate nucleation, so this may be taken as a special case where the balance of nucleation and growth is being manipulated by a chemical interaction with an additional ligand that itself does not itself form part of the crystal structure of the product.

The cases of the materials that show one-dimensional crystal also shows some interesting trends. For the Li(TPDC)(DMF) (El Osta *et al.*, 2012) and CPO-27(Ni) MOFs their crystallisations are nucleation controlled, with high activation energies for nucleation



https://doi.org/10.1017/S0885715613000997 Published online by Cambridge University Press

compared to crystals growth. For the former case, however, nucleation does not extend far into the crystallisation, leading to larger needle-like crystals. For the latter case nucleation continues into the crystallisation period leading to smaller crystals since crystal growth occurs not only at the initially formed nucleation sites but in competition with those that continue to form.

Table 2: Comparison of crystallisation data for various MOFs derived from Gualtieri fitting of crystallisation curves from *in situ* diffraction experiments (all time-resolved EDXRD studies with conventional heating). $E_a$(nuc) and $E_a$(gr) are activation energies for nucleation and growth, respectively.

| **Material** | **Nucleation** | **Crystal Morphology**[a] | **Crystal Size**[a] | $n$[b] | $E_a$**(nuc)/ kJ mol$^{-1}$** | $E_a$**(gr)/ kJ mol$^{-1}$** | **Temperature Range / $^o$C** | **Reference** |
|---|---|---|---|---|---|---|---|---|
| CPO-27(Ni) | Induction time; extended nucleation | Elongated | up to 5 μm | 1 | 132.3 | 92.3 | $90 \leq T \leq 110$ | This work |
| CPO-27(Co) | Instantaneous, short nucleation period | Elongated | ~ 10 μm | 1 | 66.5 | 90.4 | $70 \leq T \leq 100$ | This work |
| Li(TPDC)(DMF)[c] | Induction time, short nucleation | Needle | ~ 1 mm in length | 1 | 132.7 | 114.7 | $160 \leq T \leq 180$ | (El Osta *et al.*, 2012) |
| HKUST-1 (Cu) | Instantaneous and continuous | Octahedral | up to 20 μm | 3 | 71.6 | 63.8 | $85 \leq T \leq 125$ | (Millange *et al.*, 2011) |
| MOF-14 (Cu) | Instantaneous and continuous | Cubic | up to 10 μm | 3 | 113.9 | 82.8 | $110 \leq T \leq 140$ | (Millange *et al.*, 2011) |
| ZIF-8 (Zn)[d] | Short induction and continuous | Truncated cubic | greater than 20 μm | 3 | 69.0 | 71.8 | $120 \leq T \leq 140$ | (Cravillon *et al.*, 2012) |

a. Based on SEM observations of reactions allowed to reach completion; b. Dimensionality of crystal growth (see Equation 2); c. TPDC = 2,5- thiophenedicarboxylate and DMF = *N*,*N*-dimethylformamide; d. Crystallisation was studied in the presence of formate as nucleation modifier.

Finally, we compare the kinetics of microwave heated reactions with those heated using conventional means. Table III shows activation energies obtained for the microwave reactions, which can be compared directly with the values in Tables I and II. The effect of microwave heating is apparent in a lowering of the activation energies of both crystal growth for both CPO-27(Co) and CPO-27(Ni) compared to the values seen in conventional heating studies. The effect of microwave heating is also apparent on the activation energy for nucleation: both materials now have more similar values. The advantage of microwave heating in solvothermal reactions is believed to be in the high heating rate and in application of homogeneous heating: for MOF crystallisation this generally results in shorter reaction



https://doi.org/10.1017/S0885715613000997 Published online by Cambridge University Press

times and the production of smaller crystals (Stock and Biswas, 2012). In a previous study of the formation of the aluminium dihydroxyterephthalate CAU-1-$(OH)_2$ using *in situ* EDXRD, it was found that microwave heating shortened both induction time and total time of crystallisation, compared to conventional heating, although activation energy (for crystallisation, determined using an Avrami-type model) was unchanged (Ahnfeldt *et al.*, 2011). Our new results for CPO-27 show different effects of microwave heating: first, a general lower of activation energies, and, second, a change to similar crystallisation kinetics for the Ni and Co versions of the material in that activation energies for nucleation and growth follow the same trend (in contrast to conventional heating), suggesting that the lowering lability of solvated $Ni^{2+}$ is overcome. Clearly more detailed studies must be undertaken from a range of materials to obtain a systematic view of the effect of microwave heating of MOF crystallisation, but our new results provide new reference kinetic data as a basis for this work.

Table 3: Crystallisation Kinetic Parameters under Microwave Heating

| **Material** | **Nucleation** | ***n*** | **$E_a$(nuc)/ kJ mol$^{-1}$** | **$E_a$(gr)/ kJ mol$^{-1}$** | **Temperature Range / $^o$C** |
|---|---|---|---|---|---|
| CPO-27(Ni) | Instantaneous, moderate nucleation period | 1 | 72.8 | 63.8 | $80 \leq T \leq 100$ |
| CPO-27(Co) | Instantaneous, short nucleation period | 1 | 83.6 | 48.4 | $70 \leq T \leq 100$ |

## IV. CONCLUSION

We have shown how the kinetics of crystallisation of an important porous MOF material under solvothermal conditions can effectively be monitored under both conventional and microwave heating conditions using time-resolved EDXRD. By use of a simple kinetic model, developed for zeolite crystallisation, we are able to compare the crystallisation kinetics of a variety of MOF materials reported in other studies. The results we have reported provide new kinetic data to describe the crystallisation of an important family of materials and will go towards a deeper understanding of their formation mechanisms. Ultimately this



https://doi.org/10.1017/S0885715613000997 Published online by Cambridge University Press

should lead to some control over crystal growth for the targeted preparation of materials with desired crystal structure and crystal form.

## ACKNOWLEDGEMENTS

We thank DESY for provision of beamtime at HASYLAB and Professor Wolfgang Bensch (Kiel) for the loan of his heating device for the *in situ* crystallisation measurements. We are grateful to Professor Alessandro Gualtieri (Modena) for useful discussions. The research leading to these results has received funding from the European Community's Seventh Framework Programme (FP7/2007-2013) under grant agreement No. 228862.



https://doi.org/10.1017/S0885715613000997 Published online by Cambridge University Press

## REFERENCES


Ahnfeldt, T., Moellmer, J., Guillerm, V., Staudt, R., Serre, C. and Stock, N. (**2011**). "High-throughput and time-resolved energy-dispersive X-ray diffraction (EDXRD) study of the formation of CAU-1-$(OH)_2$: microwave and conventional heating," Chem.--Eur. J. **17**, 6462-6468.

Allan, P. K., Wheatley, P. S., Aldous, D., Mohideen, M. I., Tang, C., Hriljac, J. A., Megson, I. L., Chapman, K. W., De Weireld, G., Vaesen, S. and Morris, R. E. (**2012**). "Metal-organic frameworks for the storage and delivery of biologically active hydrogen sulfide," Dalton Trans. **41**, 4060-4066.

Barrer, R. M. (**1982**). *Hydrothermal Chemistry of Zeolites* (Academic Press, London).

Bloch, E. D., Murray, L. J., Queen, W. L., Chavan, S., Maximoff, S. N., Bigi, J. P., Krishna, R., Peterson, V. K., Grandjean, F., Long, G. J., Smit, B., Bordiga, S., Brown, C. M. and Long, J. R. (**2011**). "Selective binding of $O_2$ over $N_2$ in a redox-active metal-organic framework with open iron(II) coordination sites," J. Amer. Chem. Soc. **133**, 14814-14822.

Cheetham, A. K. and Mellot, C. F. (**1997**). "In situ studies of the sol-gel synthesis of materials," Chem. Mater. **9**, 2269-2279.

Cravillon, J., Schroder, C. A., Bux, H., Rothkirch, A., Caro, J. and Wiebcke, M. (**2012**). "Formate modulated solvothermal synthesis of ZIF-8 investigated using time-resolved in situ X-ray diffraction and scanning electron microscopy," CrystEngComm **14**, 492-498.

Croker, D., Loan, M. and Hodnett, B. K. (**2009**). "Kinetics and mechanisms of the hydrothermal crystallization of calcium titanate species," Cryst. Growth Des. **9**, 2207-2213.

Cundy, C. S. and Cox, P. A. (**2003**). "The hydrothermal synthesis of zeolites: History and development from the earliest days to the present time," Chem. Rev. **103**, 663-701.

Czaja, A. U., Trukhan, N. and Müller, U. (**2009**). "Industrial applications of metal-organic frameworks," Chem. Soc. Rev. **38**, 1284.

Dietzel, P. D. C., Georgiev, P. A., Eckert, J., Blom, R., Strässle, T. and Unruh, T. (**2010**). "Interaction of hydrogen with accessible metal sites in the metal-organic frameworks $M_2$(dhtp) (CPO-27-M; M = Ni, Co, Mg)," Chem. Commun. (Cambridge, U. K.) 4962-4964.

El Osta, R., Frigoli, M., Marrot, J., Medina, M. E., Walton, R. I. and Millange, F. (**2012**). "Synthesis, structure, and crystallization study of a layered lithium thiophene-dicarboxylate," Cryst. Growth Des. **12**, 1531-1537.

Farrusseng, D. (**2011**). *Metal-Organic Frameworks* (Wiley-VCH, Weinheim).

Férey, G. and Serre, C. (**2009**). "Large breathing effects in three-dimensional porous hybrid matter: facts, analyses, rules and consequences," Chem. Soc. Rev. **38**, 1380-1399.

Feyand, M., Hübner, A., Rothkirch, A., Wragg, D. S. and Stock, N. (**2012**). "Copper




https://doi.org/10.1017/S0885715613000997 Published online by Cambridge University Press

phosphonatoethanesulfonates: temperature dependent in situ energy dispersive X-ray diffraction study and influence of the pH on the crystal structures," Inorg. Chem. **51**, 12540-12547.

Feyand, M., Näther, C., Rothkirch, A. and Stock, N. (**2010**). "Systematic and in situ energy dispersive X-ray diffraction investigations on the formation of lanthanide phosphonatobutanesulfonates: $Ln(O_3P\text{-}C_4H_8\text{-}SO_3)(H_2O)$; (Ln = La-Gd)," Inorg. Chem. **49**, 11158-11163.

Francis, R. J. and O'Hare, D. (**1998**). "The kinetics and mechanisms of the crystallisation of microporous materials," J. Chem. Soc., Dalton Trans. (1972-1999) (19), 3133-3148.

Francis, R. J., Price, S. J., Evans, J. S. O., O' Brien, S., O' Hare, D. and Clark, S. M. (**1996**). "Hydrothermal synthesis of microporous tin sulfides studied by real-time in situ energy-dispersive X-ray diffraction," Chem. Mater. **8**, 2102.

Glover, T. G., Peterson, G. W., Schindler, B. J., Britt, D. and Yaghi, O. (**2011**). "MOF-74 building unit has a direct impact on toxic gas adsorption," Chem. Eng. Sci. **66**, 163-170.

Gualtieri, A. F. (**2001**) "Synthesis of sodium zeolites from a natural halloysite," Phys. Chem. Miner. **28**, 719-728.

Haque, E. and Jhung, S. H. (**2011**). "Synthesis of isostructural metal-organic frameworks, CPO-27s, with ultrasound, microwave, and conventional heating: Effect of synthesis methods and metal ions," Chem. Eng. J. (Amsterdam, Neth.) **173**, 866-872.

Horcajada, P., Gref, R., Baati, T., Allan, P. K., Maurin, G., Couvreur, P., Ferey, G., Morris, R. E. and Serre, C. (**2012**). "Metal-organic frameworks in biomedicine," Chem. Rev. **112**, 1232-1268.

Kepert, C. J. (**2010**). "Metal-Organic Framework Materials," in *Porous Materials* edited by Bruce, D. W., O'Hare, D. and Walton, R. I. (John Wiley and Sons, Chichester), pp. 1-56.

Kiebach, R., Pienack, N., Bensch, W., Grunwaldt, J. D., Michailovski, A., Baiker, A., Fox, T., Zhou, Y. and Patzke, G. R. (**2008**). "Hydrothermal formation of W/Mo-Oxides: A multidisciplinary study of growth and shape," Chem. Mater. **20**, 3022-3033.

Kiebach, R., Pienack, N., Ordolff, M. E., Studt, F. and Bensch, W. (**2006**). "Combined in situ EDXRD/EXAFS investigation of the crystal growth of $[Co(C_6H_{18}N_4)][Sb_2S_4]$ under solvothermal conditions: two different reaction pathways leading to the same product," Chem. Mater. **18**, 1196-1205.

Long, J. R. and Yaghi, O. M. (**2009**). "The pervasive chemistry of metal–organic frameworks," Chem. Soc. Rev. **38**, 1213-1214.

MacGillivray, L. R. (**2010**) *Metal-Organic Frameworks Design and Application* (John Wiley and Sons, Hoboken).

Millange, F., El Osta, R., Medina, M. E. and Walton, R. I. (**2011**). "A time-resolved diffraction study of a window of stability in the synthesis of a copper carboxylate metal-organic framework," CrystEngComm, **13**, 103-108.



https://doi.org/10.1017/S0885715613000997 Published online by Cambridge University Press

Millange, F., Medina, M., Guillou, N., Férey, G., Golden, K. M. and Walton, R. I. (**2010**). "Time-resolved in situ diffraction of the solvothermal crystallisation of some prototypical metal organic frameworks," Angew. Chem. Int. Ed. **49**, 763-766.

Modeshia, D. R., Darton, R. J., Ashbrook, S. E. and Walton, R. I. (**2009**). "Control of polymorphism in $NaNbO_3$ by hydrothermal synthesis," Chem. Commun. (Cambridge, U. K.) (1), 68-70.

Munn, J., Barnes, P., Hausermann, D., Axon, S. A. and Klinowski, J. (**1992**). "In situ studies of the hydrothermal synthesis of zeolites using synchrotron energy-dispersive X-ray-diffraction," Phase Transitions **39**, 129-134.

Murray, L. J., Dinca, M. and Long, J. R. (**2009**). "Hydrogen storage in metal-organic frameworks,". Chem. Soc. Rev. **38**, 1294-1314.

O'Hare, D., Evans, J. S. O., Fogg, A. and O'Brien, S. (**2000**). "Time-resolved, in situ X-ray diffraction studies of intercalation in lamellar hosts," Polyhedron **19**, 297-305.

OriginLabCorp (**1991-2010**) OriginPro 8.1 SR3 (Computer Software) OriginLabCorp, Northhampton MA.

Pienack, N. and Bensch, W. (**2011**). "In-situ monitoring of the formation of crystalline solids," Angew. Chem.-Int. Edit. **50**, 2014-2034.

Reinsch, H. and Stock, N. (**2012**). "Formation and characterization of Mn-MIL-100," CrystEngComm (3), 544-550.

Rosi, N. L., Kim, J., Eddaoudi, M., Chen, B. L., O'Keeffe, M. and Yaghi, O. M. (**2005**). "Rod packings and metal-organic frameworks constructed from rod-shaped secondary building units," J. Am. Chem. Soc **127**, 1504-1518.

Rothkirch, A. (**2009**). f3tool version 0.3b (18.11.2009) (Computer Software), Beamline F3, Hasylab (DESY).

Sankar, G., Okubo, T., Fan, W. and Meneau, F. (**2007**). "New insights into the formation of microporous materials by in situ scattering techniques" Faraday Discuss. **136**, 157-166.

Schmidt, C., Feyand, M., Rothkirch, A. and Stock, N. (**2012**). "High-throughput and in situ EDXRD investigation on the formation of two new metal aminoethylphosphonates - $Ca(O_3PC_2H_4NH_2)$ and $Ca(OH)(O_3PC_2H_4NH_3)$ $2H_2O$," J. Solid State Chem. **188**, 44-49.

Schmidt, C. and Stock, N. (**2012**). "Systematic investigation of zinc aminoalkylphosphonates: influence of the alkyl chain lengths on the structure formation," Inorg. Chem. **51**, 3108--3118.

Shoaee, M., Agger, J. R., Anderson, M. W. and Attfield, M. P. (**2008**). "Crystal form, defects and growth of the metal organic framework HKUST-1 revealed by atomic force microscopy," CrystEngComm **10**, 646-648.

Stavitski, E., Goesten, M., Juan-Alcaniz, J., Martinez-Joaristi, A., Serra-Crespo, P., Petukhov, A. V.,



https://doi.org/10.1017/S0885715613000997 Published online by Cambridge University Press

Gascon, J. and Kapteijn, F. (**2011**). "Kinetic control of metal-organic framework crystallization investigated by time-resolved in situ X-ray scattering," Angew. Chem., Int. Ed. **50**, 9624-9628.

Stock, N. and Biswas, S. (**2012**). "Synthesis of metal-organic frameworks (MOFs): routes to various MOF topologies, morphologies, and composites," Chem. Rev. **112**, 933-969.

Sumida, K., Rogow, D. L., Mason, J. A., McDonald, T. M., Bloch, E. D., Herm, Z. R., Bae, T. H. and Long, J. R. (**2012**). "Carbon dioxide capture in metal-organic frameworks," Chem. Rev. **112**, 724-781.

Walton, R. I., Francis, R. J., Halasyamani, P. S., O' Hare, D., Smith, R. I., Done, R. and Humphreys, R. J. (**1999a**). "Novel apparatus for the in situ study of hydrothermal crystallizations using time-resolved neutron diffraction," Rev. Sci. Instrum. **70**, 3391-3396.

Walton, R. I., Loiseau, T., O'Hare, D. and Férey, G. (**1999b**). "An in situ energy-dispersive X-ray diffraction study of the crystallisation of open-framework gallium oxyfluorophosphates with the ULM-3 and ULM-4 structure," Chem. Mater. **11**, 3201-3209.

Walton, R. I., Millange, F., O'Hare, D., Davies, A. T., Sankar, G. and Catlow, C. R. A. (**2001**). "An in situ energy-dispersive X-ray diffraction study of the hydrothermal crystallisation of zeolite A. 1. influence of reaction conditions and transformation into sodalite," J. Phys. Chem. B. **101**, 83-90.

Walton, R. I. and O'Hare, D. (**2000**). "Watching solids crystallise using in situ powder diffraction," Chem. Commun. (Cambridge, U. K.) (23), 2283-2291.

Yaghi, O. M., O'Keeffe, M., Ockwig, N. W., Chae, H. K., Eddaoudi, M. and Kim, J. (**2003**). "Reticular synthesis and the design of new materials," Nature **423**, 705-714.

Yoon, M., Srirambalaji, R. and Kim, K. (**2012**). "Homochiral metal-organic frameworks for asymmetric heterogeneous catalysis," Chem. Rev. **112**, 1196-1231.

Zacher, D., Liu, J. N., Huber, K. and Fischer, R. A. (**2009**). "Nanocrystals of $Cu_3(btc)_2$ (HKUST-1): a combined time-resolved light scattering and scanning electron microscopy study," Chem. Commun. (Cambridge, U. K.) (9), 1031-1033.



https://doi.org/10.1017/S0885715613000997 Published online by Cambridge University Press